

# MICROSTRUCTURE AND RED LUMINESCENCE OF ZnO NANOPARTICLES/NANOFIBERS SYNTHESIZED BY ELECTROSPINNING FOLLOWED BY THERMAL ANNEALING\*\*

P. V. Huan<sup>1</sup>, N. D. Thong<sup>1,2</sup>, V. T. P. Thuy<sup>1,3</sup>, L. V. Toan<sup>1,4</sup>,  
N. D. T. Kien<sup>1</sup>, T. Q. Tuan<sup>1\*</sup>, V.-H. Pham<sup>1\*</sup>

<sup>1</sup> Advanced Institute for Science and Technology (AIST) at Hanoi University of Science and Technology (HUST) Hanoi, Vietnam; e-mail: [vuong.phamhung@hust.edu.vn](mailto:vuong.phamhung@hust.edu.vn), [tuan.taquoc@hust.edu.vn](mailto:tuan.taquoc@hust.edu.vn)

<sup>2</sup> School of Engineering Physics at Hanoi University of Science and Technology (HUST), Hanoi, Vietnam

<sup>3</sup> Trade Union University, Hanoi, Vietnam

<sup>4</sup> Le Quy Don Technical University, Hanoi, Vietnam

*This paper reports the red visible luminescence of ZnO nanofibers synthesized by electrospinning followed by thermal annealing. The ZnO nanofibers were prepared by electrospinning of the precursor mixture of zinc acetate/polyvinylpyrrolidone (PVP) by using different PVP concentrations, while thermal annealing was kept at 600°C. The ZnO nanofiber diameter was dependent on the PVP concentrations, which increased as PVP concentrations increased. Thermal annealing induced significant changes in ZnO nanofibers, which formed ZnO nanoparticle/nanofiber structures as a function of PVP concentrations. The ZnO nanofibers synthesized with PVP concentration of 20% induced homogeneous distribution of ZnO nanoparticles with highly visible luminescence intensities centering at ~650 nm. Results indicated that the use of electrospinning followed by thermal annealing could be an important method for the synthesis of ZnO nanoparticle/nanofiber structures, which could be used in advanced engineering such as optoelectronics and sensing.*

**Keywords:** nanofiber, luminescence, ZnO, visible-light, nanoparticles.

# МИКРОСТРУКТУРА И КРАСНАЯ ЛЮМИНЕСЦЕНЦИЯ НАНОЧАСТИЦ/НАНОВОЛОКОН ZnO, СИНТЕЗИРОВАННЫХ МЕТОДОМ ЭЛЕКТРОВЫТЯГИВАНИЯ С ПОСЛЕДУЮЩИМ ТЕРМИЧЕСКИМ ОТЖИГОМ

P. V. Huan<sup>1</sup>, N. D. Thong<sup>1,2</sup>, V. T. P. Thuy<sup>1,3</sup>, L. V. Toan<sup>1,4</sup>,  
N. D. T. Kien<sup>1</sup>, T. Q. Tuan<sup>1\*</sup>, V.-H. Pham<sup>1\*</sup>

УДК 535.37;620.3

<sup>1</sup> Передовой институт науки и техники (AIST) при Ханойском университете науки и техники (HUST) Ханой, Вьетнам; e-mail: [vuong.phamhung@hust.edu.vn](mailto:vuong.phamhung@hust.edu.vn), [tuan.taquoc@hust.edu.vn](mailto:tuan.taquoc@hust.edu.vn)

<sup>2</sup> Школа инженерной физики Ханойского университета науки и техники (HUST), Ханой, Вьетнам

<sup>3</sup> Университет профсоюзов, Ханой, Вьетнам

<sup>4</sup> Технический университет Ле Куи Дона, Ханой, Вьетнам

(Поступила 18 мая 2020)

*Изучена красная видимая люминесценция нановолокон ZnO, синтезированных методом электровытягивания с последующим термическим отжигом при температуре 600 °C. Нановолокна ZnO получены путем электровытягивания смеси предшественника ацетата цинка — поливинилпирролидона (ПВП), с использованием различных концентраций ПВП. Диаметр нановолокна ZnO зависит от концентрации ПВП и увеличивается по мере роста концентрации ПВП. Термический отжиг вызывает значительные изменения в нановолокнах ZnO, которые формируют структуры наночастиц/нановолокон ZnO в зависимости от концентрации ПВП. Нановолокна ZnO, синтезированные с концентрацией ПВП 20 %, индуцируют однородное распределение наночастиц ZnO с высокой ин-*

\*\*Full text is published in JAS V. 88, No. 4 (<http://springer.com/journal/10812>) and in electronic version of ZhPS V. 88, No. 4 ([http://www.elibrary.ru/title\\_about.asp?id=7318](http://www.elibrary.ru/title_about.asp?id=7318); [sales@elibrary.ru](mailto:sales@elibrary.ru)).

тенсивностью видимой люминесценции вблизи ~650 нм. Показано, что электровытягивание с последующим термическим отжигом может быть важным методом синтеза наночастиц ZnO/нано-волоконных структур, которые могут применяться в передовой технике — оптоэлектронике и зондировании.

**Ключевые слова:** нановолокно, люминесценция, ZnO, видимый свет, наночастица.

**Introduction.** The development of new nanostructure materials for tuning the properties is an interesting research area in nanotechnology [1, 2]. This research area has encouraged scientists and engineers to explore new ways of designing microstructure by tailoring the physical and chemical characteristics of materials, for example, by creating heterostructures of materials in the nanoscale level [3, 4]. As a one-dimensional material, ZnO nanofibers have received considerable attention in optoelectronic materials because of its wide band gap semiconductor, large excitation binding energy of 60 meV, biocompatible materials, lower cost of manufacture, and chemical stability [5, 6]. Luminescence of ZnO has been observed in two typical emission bands: an ultraviolet near-band-edge (NBE) emission caused by the recombination of free excitons through exciton–exciton collision, and visible-light emission caused by the defect in ZnO [7, 8]. Most syntheses of ZnO showed NBE and visible emission under certain excitation energy. However, controlling a single specific emission center of ZnO is of particular interest in optoelectronics and optical sensing. A previous document demonstrated that NBE emission of ZnO could be obtained by the existence of a highly crystalline ZnO nanostructure [9, 10]. Other research literature revealed that visible-light emission of ZnO was achieved by forming an oxygen or Zn interstitial defect in ZnO [11, 12]. Most defect-induced visible-light emission of ZnO is centered at ~530 nm [13, 14]. Few publications reported visible-light emission of ZnO in the red range (610–700) of spectrum [15, 16]. Therefore, this study reports for the first time the red visible-light emission of ZnO centering at ~650 nm by forming ZnO nanoparticle/nanofiber structures, which can be achieved by electrospinning followed by thermal annealing in air. Electrospinning is a unique method to synthesize nanofibers [17]. In this method, the feed solution is exposed to high voltage up to 10 kV through the needle, leading to the formation of nanofibers under the Taylor cone as the electric field strength exceeds the surface tension of the liquid [18]. The microstructure and crystal structure of the nanowires are characterized by field emission scanning electron microscopy (FESEM) and X-ray diffraction (XRD), respectively. Light emission of the ZnO nanofibers was determined using a photoluminescence (PL) spectrometer.

**Experimental procedure.** ZnO nanofibers were synthesized by electrospinning of the precursor mixture containing zinc acetate (99.99%, Sigma-Aldrich)/polyvinylpyrrolidone (PVP, 99.9%, Sigma-Aldrich) at room temperature. A series of ZnO nanofibers was synthesized by electrospinning (Electrospunra, Singapore) using 2.5 g of zinc acetate dissolved in 10 mL of ethanol. Then various weight (wt) amounts of PVP in the range of 15, 20, 25, and 30% were added into the solution to control the microstructure of the ZnO nanofibers. The solution was stirred for 6 h at room temperature to obtain homogeneous solution. The as-prepared solution was transferred to a plastic syringe with a stainless steel needle. High voltage of 15 kV was applied to the electrospinning system, and ZnO nanofibers were formed on aluminum foil. ZnO nanofibers were pulled out from the aluminum foil and placed in a ceramic boat for thermal annealing. The specimens were placed inside the furnace (Nabertherm, Germany), which was adjusted to 600°C at a heating rate of 10°C min<sup>-1</sup> for 2 h in ambient atmosphere. After that, the system was naturally cooled to room temperature for the formation of ZnO nanoparticle/nanofiber structures. The crystal structure of the ZnO nanofibers was characterized by XRD (D8 Advance, Bruker, Germany). The microstructure of the ZnO nanofibers was determined by FESEM (JEOL, JSM-7600F, JEOL Techniques, Tokyo, Japan) and HRTEM (JEM 2100, JEOL Techniques, Tokyo, Japan). Chemical composition and chemical bonding of the ZnO nanofibers were analyzed by energy-dispersive X-ray spectroscopy (EDS, Gatan, UK) and Fourier transform infrared spectrometry using a Perkin-Elmer Spectrum BX spectrometer and KBr pellets. Room-temperature photoluminescence (PL) tests were performed to evaluate the physical properties of the ZnO nanofibers. A NANO LOG spectrofluorometer (Horiba, USA) equipped with a 450 W Xe arc lamp and double excitation monochromators was used.

**Results and discussion.** *Phase characterization.* Figures 1 shows the typical XRD patterns of the ZnO nanofibers prepared by electrospinning with a PVP concentration of 20% followed by annealing at 600°C. The ZnO nanofibers showed several strong peaks at  $2\theta = 31.8^\circ, 34.4^\circ, 36.1^\circ, 47.4^\circ, 56.50^\circ, 62.80^\circ, 66.54^\circ,$  and  $67.88^\circ$ , which were characterized by the (100), (002), (101), (102), (110), (103), (200), and (112) planes of the crystalline hexagonal wurtzite ZnO phase, respectively (JCPDS 36-1451). The XRD patterns showed that good crystallinity was represented by high peak intensity and narrow peak spectra, which was often the case with ZnO nanofibers synthesized by electrospinning followed by thermal annealing [19, 20].

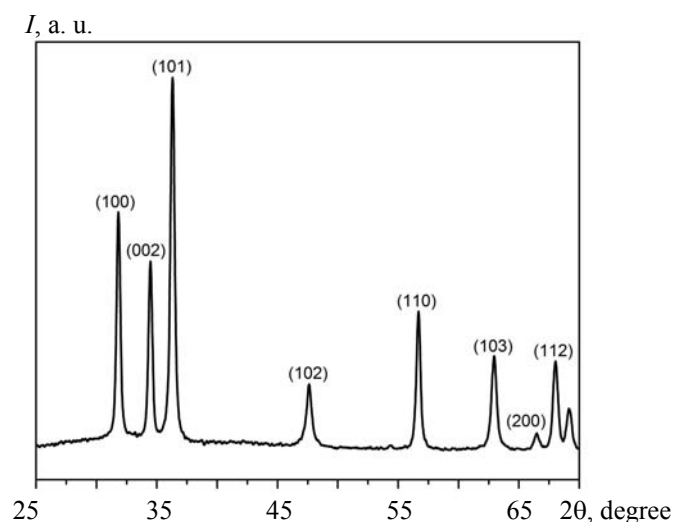


Fig. 1. XRD patterns of ZnO nanofibers prepared by electrospinning with a PVP concentration of 20% followed by thermal annealing at 600°C.

*Scanning electron analysis.* The microstructure variation in ZnO nanofibers synthesized by electrospinning with different concentrations of PVP was investigated by SEM (Figs. 2a–d). The specimens prepared with PVP concentration of 15% showed a nanofiber structure with a diameter of ~200 nm and several micrometers in length (Fig. 2a). When the amount of PVP increased to 20%, the specimens still displayed nanofiber morphology with a slightly increased diameter (Fig. 2b). On the contrary, the increase in nanofiber morphology became clear with a diameter of ~300 nm as the amount of PVP increased to 25% (Fig. 2c). The increase in nanofiber diameter became vigorous as the amount of PVP increased to 30%, while the fiber diameter increased to ~350 nm (Fig. 2d). This increase in ZnO nanofiber diameter was attributed to the increase in viscosity when a high concentration of PVP was used [20, 21].

Figure 2 shows the microstructure of ZnO nanofibers synthesized by electrospinning with different PVP concentrations followed by thermal annealing at 600°C. ZnO nanofibers consist of a homogeneous distribution of ZnO nanoparticles with a diameter of ~20 nm when 15% PVP was used (Fig. 2a'). When the amount of PVP increased to 20%, the ZnO nanofibers displayed a homogeneous distribution of ZnO nanoparticles with slightly increased ZnO nanoparticle size (Fig. 2b'). ZnO nanofibers became rough when the ZnO nano-

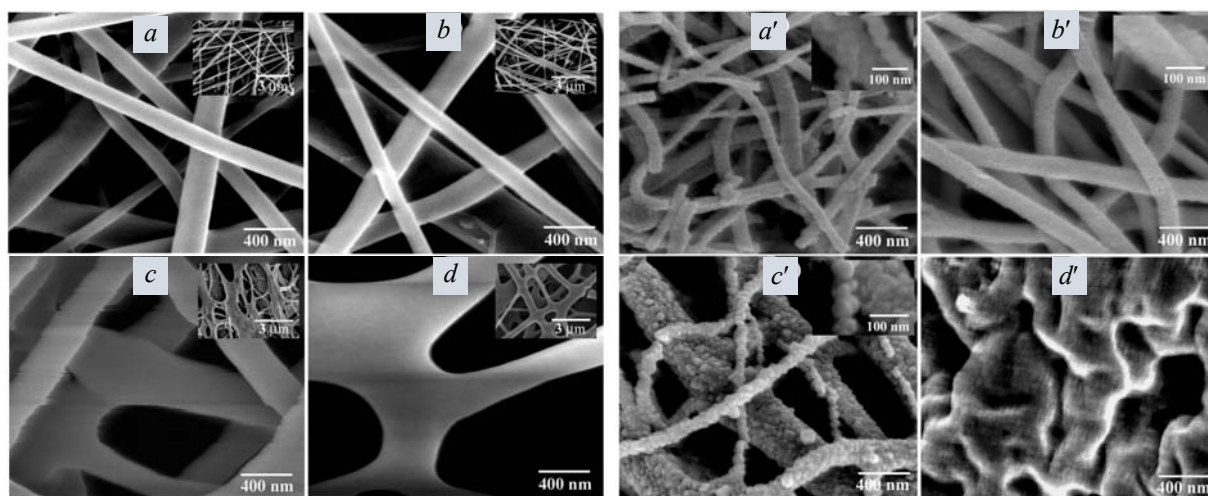


Fig. 2. SEM image of ZnO nanofibers synthesized by electrospinning using different PVP concentrations: (a, a') 15%, (b, b') 20%, (c, c') 25%, and (d, d') 30% without annealing (a–d) and followed by thermal annealing at 600°C (a'–d').

particle size increased to ~50 nm, thereby increasing the amount of PVP to 25% (Fig. 2c'). This finding indicated that the microstructure of ZnO nanofibers could be controlled by changing the initial concentration of PVP followed by thermal annealing. However, evidence of ZnO nanoparticles was not observed in ZnO nanofibers when the PVP concentration increased to 30% (Fig. 2d'). The formation of ZnO nanoparticles on the nanofiber skeleton could be attributed to the evaporation of PVP polymer during thermal annealing [22, 23]. Based on previous reports, the high viscosity solution from the high concentration of PVP could result in increased binding of the Zn-based precursor and larger nanoparticle size of ZnO.

**Chemical composition analysis.** The representative chemical composition of the ZnO nanofibers was characterized by EDS (Fig. 3). The peaks corresponding to Zn and oxygen elements with an atomic ratio of ~1:1 was observed, confirming the formation of ZnO. The Si and Pt peaks in the EDS spectrum were attributed to the ZnO nanofibers attaching on the Si substrate and Pt coating for good SEM coupling with EDS analysis.

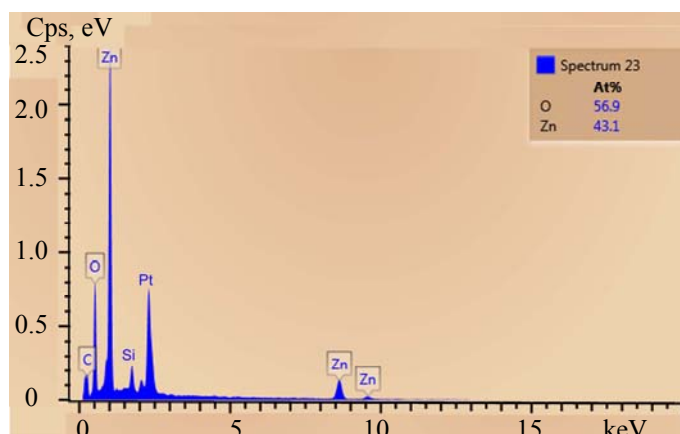


Fig. 3. EDS analysis of ZnO nanofibers with PVP concentrations of 20% annealed at 600°C.

**Microstructural analysis.** Further structural characterization of the ZnO nanofibers was performed by TEM. A low-magnification TEM image showed that small ZnO nanoparticles were connected with one another as building units to form ZnO nanofibers (Fig. 4a). Figure 4b shows an HRTEM analysis of the ZnO nanoparticles, in which the 0.2476 nm crystal plane spacing is assigned to ZnO (101).

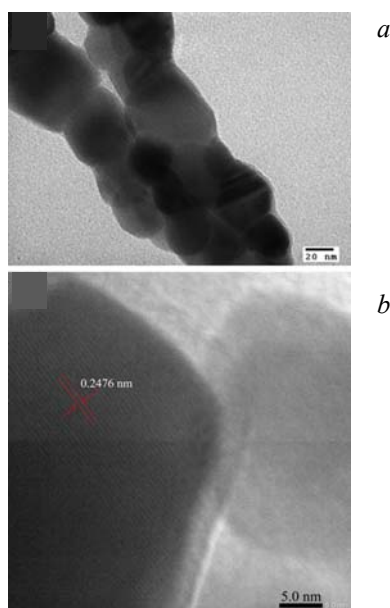


Fig. 4. (a) Low-magnification TEM image of ZnO nanofibers; (b) HRTEM image of crystalline ZnO nanofibers with PVP concentrations of 20% annealed at 600°C.

**Photoluminescence analysis.** Figure 5 shows the emission spectra of ZnO nanofibers with different PVP concentrations annealed at 600°C and monitored at 280 nm. All PL signals showed strong visible emission peaks at ~650 nm with a suppressed NBE emission of ~380 nm. PL intensities of ZnO nanofibers increased with increase in the amount of PVP during electrospinning; that is, when the amount of PVP reached 20%, PL intensities reached the maximum value. However, PL intensities decreased when PVP concentration was further increased. Previous documents demonstrated that the visible emission band from ZnO was due to the interstitial oxygen defect of ZnO during thermal annealing [24–26]. Here, a dominant visible band was observed, indicating that interstitial oxygen defects were also present in the ZnO nanofibers. The formation of defect could originate from the evaporation of PVP during thermal annealing at 600°C. The high concentration of ZnO nanoparticles/surfaces in ZnO nanofibers could introduce a relatively high number of defects at the surface and interface to form defect energy bands, which could trap free carriers from the fibers, resulting in highly visible emission. With increase in PVP concentration, the increasing ZnO nanoparticle size could lead to a small surface-to-volume ratio, which could be decreased in the visible emission intensity.

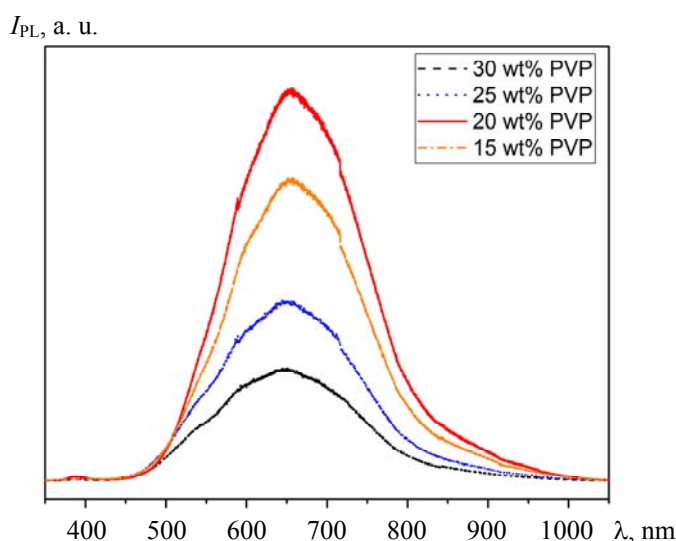


Fig. 5. Photoluminescence spectra of ZnO nanofibers synthesized by electrospinning using different PVP concentrations followed by thermal annealing at 600°C.

**Conclusions.** We demonstrated that the stabilization of visible-light emission from ZnO nanofibers could be obtained effectively by electrospinning followed by thermal annealing. In particular, the microstructure of ZnO was controlled by using different PVP concentrations, that is, the formation of ZnO nanoparticle/nanofiber structures. Moreover, these ZnO nanoparticle/nanofiber structures could achieve a unique emission band at ~650 nm with controllable intensities. These findings indicate that the present method is important in the fabrication of ZnO nanoparticle/nanofiber structures, which are important for designing optical properties in the field of optoelectronics and sensing.

**Acknowledgments.** This research is funded by Hanoi University of Science and Technology (HUST) under grant number T2018-PC-201.

## REFERENCES

1. Z. R. Dai, Z. W. Pan, Z. L. Wang, *Adv. Funct. Mater.*, **13**, 9–24 (2013).
2. J. Lian, Z. Ding, F. L. Kwong, D. H. L. Ng, *Cryst. Eng. Commun.*, **13**, 4820–4822 (2011).
3. Q. Tang, W. Zhou, J. Shen, W. Zhang, L. Kong, Y. Qian, *Chem. Commun.*, **10**, 712–713 (2004).
4. M. McCune, W. Zhang, Y. Deng, *Nano Lett.*, **12**, 3656–3662 (2012).
5. D. Yuvaraj, K. Narasimha Rao, K. Barai, *Solid State Commun.*, **149**, 349–351 (2009).
6. W. Wang, B. Zeng, J. Yang, B. Poudel, J. Huang, M. J. Naughton, Z. Ren, *Adv. Mater.*, **18**, 3275–3278 (2006).

7. V. H. Pham, V. T. Kien, P. D. Tam, P. T. Huy, *Mater. Sci. Eng: B*, **209**, 17–22 (2016).
8. S. Cho, J. Ma, Y. Kim, Y. Sun, G. K. L. Wong, J. B. Ketterson, *Appl. Phys. Lett.*, **75**, 2761 (1999).
9. A. Umar, B. K. Kim, J. J. Kim, Y. B. Hahn, *Nanotechnology*, **18**, 175606 (2007).
10. S. S. Warule, N. S. Chaudhari, B. B. Kale, M. A. More, *Cryst. Eng. Comm.*, **11**, 2776–2783 (2009).
11. V. Kumar, V. Kumar, S. Som, A. Yousif, N. Singh, O. M. Ntwaeaborwa, A. Kapoor, H. C. Swart, *J. Colloid Interf. Sci.*, **428**, 8–15 (2014).
12. H. Q. Wang, G. Z. Wang, L. C. Jia, C. J. Tang, G. H. Li, *J. Phys. D: Appl. Phys.*, **40**, 6549–6553 (2007).
13. D. Y. Jiang, J. X. Zhao, M. Zhao, Q. C. Liang, S. Gao, J. M. Qin, Y. J. Zhao, A. Li, *J. Alloys Compd.*, **532**, 31–33 (2012).
14. D. H. Fan, W. Z. Shen, M. J. Zheng, Y. F. Zhu, J. J. Lu, *J. Phys. Chem. C*, **111**, 9116–9121 (2007).
15. R. Raji, K. G. Gopchandran, *J. Sci.: Adv. Mater. Devic.*, **2**, 51–58 (2017).
16. A. B. Djurišić, Y. H. Leung, K. H. Tam, L. Ding, W. K. Ge, H. Y. Chen, S. Gwo, *Appl. Phys. Lett.*, **88**, 103107 (2006).
17. M. Kitsara, O. Agbulut, D. Kontziampasis, Y. Chen, P. Menasché, *Acta Biomater.*, **48**, 20–40 (2017).
18. Travis J. Sill, Horst A. von Recum, *Biomaterials*, **29**, 1989–2006 (2008).
19. C. Lai, X. Wang, Y. Zhao, H. Fong, Z. Zhu, *RSC Adv.*, **3**, 6640–6645 (2013).
20. E. Ghafari, Y. Feng, Y. Liu, I. Ferguson, N. Lu, *Composites Part B*, **116**, 40–45 (2017).
21. H. Wu, W. Pan, *J. Am. Ceram. Soc.*, **89**, 699–701 (2006).
22. J. Y. Park, S. S. Kim, *J. Am. Ceram. Soc.*, **92**, 1691–1694 (2009).
23. D. Y. Leea, J. E. Choa, N. I. Chob, M. H. Leec, S. S. J. Leed, B. Y. Kim, *Thin Solid Films*, **517**, 1262–1267 (2008).
24. A. Baez-Rodríguez, L. Zamora-Peredo, M. G. Soriano-Rosales, J. Hernandez-Torres, L. García-González, R. M. Calderón-Olvera, M. García-Hipólito, J. Guzmán-Mendoza, C. Falcony, *J. Lumin.*, **218**, 116830 (2020).
25. J. Zhou, K. Nomenyo, C. C. Cesar, A. Lusson, A. Schwartzberg, C. C. Yen, W. Y. Woon, G. Leronde, *Sci. Rep.*, **10**, 4237 (2020).
26. Y. Kumar, A. K. Rana, P. Bhojane, M. Pusty, V. Bagwe, S. Sen, P. M. Shirage, *Mater. Res. Express*, **2**, 105017 (2015).